

Bulk Electronic Structure of Ni_2MnGa studied by Density Functional Theory and Hard X-ray Photoelectron Spectroscopy

Joydipto Bhattacharya^{1,2,†}, Pampa Sadhukhan^{3,†}, Shuvam Sarkar³, Vipin Kumar Singh³, Andrei Gloskovskii⁴, Sudipta Roy Barman¹, and Aparna Chakrabarti^{1,2}

¹*Homi Bhabha National Institute, Training School Complex, Anushakti Nagar, Mumbai 400094, India*

²*Raja Ramanna Centre for Advanced Technology, Indore 452013, India*

³*UGC-DAE Consortium for Scientific Research, Khandwa Road, Indore 452001, India*

⁴*Deutsches Elektronen-Synchrotron DESY, Notkestrasse 85, D-22607 Hamburg, Germany and*

[†]*Both the authors contributed equally.*

A combined study employing density functional theory (DFT) using the experimentally determined modulated structures and bulk-sensitive hard x-ray photoelectron spectroscopy on single-crystalline Ni_2MnGa is presented in this work. For the aforementioned modulated structures, all of the characteristic features in the experimental valence band (VB) are in excellent agreement with the theoretical VB calculated from DFT, evincing that it is the true representation of Ni_2MnGa in the martensite phase. We establish the existence of a charge density wave (CDW) state in the martensite phase from the shape of the VB near E_F that shows a transfer of spectral weight in excellent agreement with DFT. Furthermore, presence of a pseudogap is established by fitting the near E_F region with a power law function predicted theoretically for the CDW phase. Thus, the present work emphasizes that the atomic modulation plays an important role in hosting the CDW phase in bulk stoichiometric Ni_2MnGa .

In recent years, considerable research has focused on understanding the intriguing physical phenomena connected to the charge density wave (CDW) state [1–5]. CDW is a collective excitation with periodic lattice distortion or modulation that often results in a pseudogap at E_F [6–8] and has been observed in various chalcogenide systems [9–11]. Ni_2MnGa is an intriguing Heusler alloy having topologically protected nontrivial spin structures, such as skyrmions [12], where the nature of atomic rearrangements related to existence of a bulk CDW state in the martensite phase has been a topic of intense study over the past three decades, but remains unresolved until date [13–30]. In addition, Ni_2MnGa is of practical importance due to its large magneto-caloric effect [31, 32] and magnetic field induced strain (MFIS) of approximately 10% [33, 34], the latter of which has been correlated with its large magnetocrystalline anisotropy [35] and low twinning stress in the low temperature martensite phase.

It was observed quite early on that the martensite phase is not a simple tetragonal distortion of the high temperature cubic (austenite) phase, rather the structure has a periodic modulation. Using powder neutron diffraction Brown *et al.* could account for all the reflections using a 7-fold supercell (7M) with a commensurate wave vector [q_{CDW}] of $\frac{3}{7}c^*$ i.e. $0.4286c^*$ [14]. The modulation results from a periodic shuffling of (110) planes of the cubic phase along the $[1\bar{1}0]$ direction. Later on, structural studies using high resolution x-ray diffraction (XRD) [15, 16] showed that the martensite phase has a sinusoidal modulation in the positions of all the three elemental constituents indicating formation of CDW with q_{CDW} of $0.425c^*$. Significantly, from inelastic neutron diffraction study [21], the martensite phase was reported to be distorted by transverse modulation with incommensurate wave vector close to that reported from XRD [15, 16] that was attributed to electron-phonon in-

teractions and anharmonic effects. A phason excitation was observed in the martensite phase of Ni_2MnGa from the neutron scattering experiment that was related to a CDW state [20]. Evidence of modulation in the martensite phase of Ni_2MnGa was also observed in electron and x-ray diffraction studies from the appearance of the satellite spots [17, 25, 26] - as is well known for chalcogenide materials that exhibit CDW [36, 37]. From a ultraviolet photoemission spectroscopy (UPS) study [13], existence of CDW in the pre-martensite phase [38] was shown on the surface of $\text{Ni}_2\text{MnGa}(100)$ that continued to exist also in the martensite phase. However, UPS being a highly surface sensitive technique with inelastic mean free path (IMFP) of 5Å, the presence of CDW could not be inferred for the bulk martensite phase and the role of modulation was not probed. A time-resolved experiment identified a coherent phonon that was related to the amplitude of the modulated structure [23]. From an *ab initio* theoretical study, Bungaro *et al.* revealed that the dynamical instability in the TA2 phonon mode is connected with the nesting of the Fermi surface [18], which is regarded as the distinguishing feature of the CDW state. Another first-principles study by Zayak *et al.* reported that the martensite phase is stabilized by modulation that showed a tendency to exhibit a pseudogap [19]; the modulated structure was close to that reported in Ref. 17.

The martensite phase of Ni_2MnGa is further complicated by non-stoichiometry, which has a substantial influence on its physical characteristics [39–42]. For example, for a composition of $\text{Ni}_{54.8}\text{Mn}_{22}\text{Ga}_{23.2}$ i.e., $\text{Ni}_{2.19}\text{Mn}_{0.88}\text{Ga}_{0.93}$, the modulated phase is not observed and the structure is tetragonal [28, 41]. For this composition, a 14M nanotwin model of the adaptive martensite phase was suggested by Kaufmann *et al.* [28]. Similarly, signature of nanotwins from transmission electron microscopy (TEM) was obtained for non-stoichiometric

compositions that exhibit martensite phase at room temperature [27], whereas Ni_2MnGa exhibits the martensite phase below the martensite finish temperature of 205 K [43]. Our survey of literature indicates that in compositions where the martensite phase has non-modulated tetragonally distorted Bain transition, the adaptive phase model [28] is applicable. However, a relatively recent density functional theory calculation shows that even for stoichiometric bulk Ni_2MnGa the modulation originates from the nanotwin ordering [29]. The authors establish that the phonon softening in the cubic austenite phase initializes the movement of the lattice planes, which seamlessly results in a nanotwinned adaptive martensite phase. However, this proposition is not supported by the conclusions of a large number of theoretical and experimental studies discussed above [13–26]. In particular, the nanotwin structure [28] was ruled out for stoichiometric Ni_2MnGa from high resolution XRD study based on inhomogeneous displacements of the different atomic sites and the presence of phason broadening [16]. In spite of the above mentioned studies indicating formation of CDW in stoichiometric bulk Ni_2MnGa [13–26], a very recent theoretical study on Ni_2MnGa using quasiparticle self-consistent GW (QS GW) method supports the formation of the 14M nanotwinned phase and thus raises doubt about the existence of the periodic modulation and the CDW state in this system [30].

In this paper, using a combination of density functional theory (DFT) and hard x-ray photoelectron spectroscopy (HAXPES), we investigate the bulk electronic structure of Ni_2MnGa in order to firmly settle the aforementioned disagreement in the literature. We perform DFT calculations utilizing the actual experimental structures [14–16], unlike previous theoretical investigations that used only non-modulated and model structures [19, 29, 30, 44, 45]. We also conducted DFT calculations utilizing the model nanotwin structure [28] in order to compare with the modulated structures. Due to the development of high brilliance synchrotron sources working in the stable top-up mode [46], HAXPES has turned out to be a useful technique to probe the bulk electronic structure [47–52]. Although there are a few HAXPES studies on other Heusler alloys [53–55], the only work on Ni-Mn-Ga system is a comparison of two non-stoichiometric compositions with widely differing martensite transition temperature and electron to atom ratios [56]. Thus, this work is not related to our current investigation on stoichiometric Ni_2MnGa in the austenite (300 K) and martensite phase (50 K) employing HAXPES and also DFT. In fact, the HAXPES study of the valence band (VB), in particular near the Fermi level (E_F), would not only throw light on the CDW state, but also act as the “gold standard” for the DFT results to ascertain which structure best characterizes the martensite phase of Ni_2MnGa .

HAXPES and DFT VB spectra in the austenite phase:

In Fig. 1(a), we compare the theoretical and experimen-

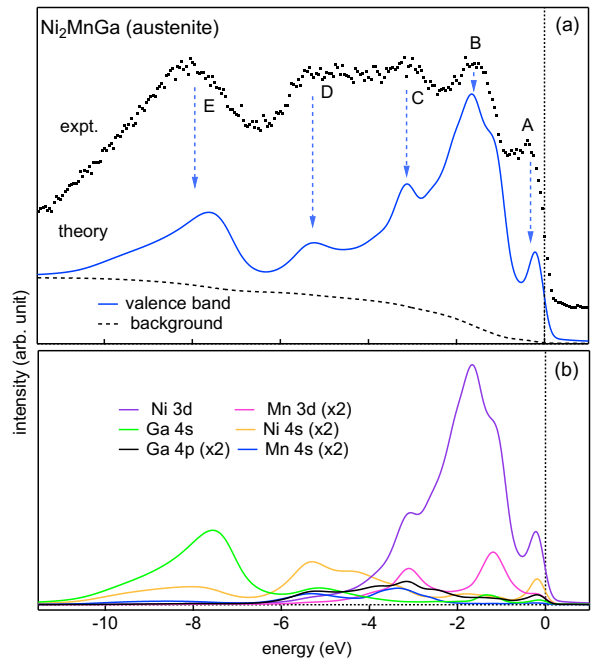


Figure 1. (a) The experimental HAXPES VB spectra of Ni_2MnGa in the austenite phase taken with 6 keV photon energy compared with the theoretical VB spectrum calculated from the partial DOS. Features **A** to **E** are marked by blue dashed arrows. The zero in the energy scale corresponds to the Fermi level (E_F). (b) The partial atom and orbital projected components of the theoretical VB.

tal VB for the austenite phase of Ni_2MnGa with $L2_1$ structure [57] [see Table S1 for its structural parameters, also Fig. S1 of the Supplementary material (SM) [58] for the structure]. The HAXPES VB spectrum exhibits five distinct features at about -0.25 (**A**), -1.6 (**B**), -3.2 (**C**), -5.35 (**D**), and -8 eV (**E**). These features are the signatures of the bulk electronic structure since HAXPES is a bulk sensitive technique with an IMFP of 66 Å (84 Å) at 6 (8) keV [59].

In order to compare with the experiment, we have calculated the VB spectrum considering the s , p , and d orbital projected components of the partial density of states (PDOS) of Ni, Mn, and Ga considering their respective photoemission cross-sections [60] [see the Methods section in SM [58] for details of the theory and experiment]. In Fig. 1(b), some of the dominant partial contributions to the calculated total VB spectrum [blue curve in Fig. 1(a)] are shown. As shown by the blue dashed arrows in Fig. 1(a), the energy positions of the features in the experimental spectra are in good agreement with the calculated VB spectra.

The sharp peak shown by **A** corresponds to the feature a_1 , observed in the theoretical DOS [see Note A and Fig. S2 in SM [58]]. This arises due to the Ni 3d minority states, with some admixture of the Ni 4s states, with minor contribution from Mn and Ga states. The intense

peak **B** is dominated by Ni 3*d* majority and minority spin states, which corresponds to feature c_1 at ~ -1.7 eV. A hump is observed at the lower binding energy side of **B** at about -1.1 eV [feature b_1]. This has major contributions from Mn 3*d* majority spin states and also from the Ni 3*d* states in both the spin channels. Feature **C** is primarily due to the Ni 3*d* states, with significant contributions from the Mn 3*d* up states, additionally, Ga 4*p* and Ni as well as Mn 4*s* states also contribute. While **E** has a dominant contribution from Ga 4*s*, with some admixture of Ni 4*s* states, **D** mainly arises from Ni 4*s* states hybridized with Ga 4*s*, Mn 4*s*, and Ga 4*p* states. A comparison of the HAXPES spectra taken with 6 and 8 keV shows that all the features **A-E** occur at similar energies [Fig. S3 of SM [58]]. Note that larger photoemission cross-section of the *s* states in HAXPES leads to appearance of features **C-E** in contrast to low energy phototemission such as x-ray photoelectron spectroscopy (XPS), where **C**, **D** are not visible and **E** is weak [43]. In Fig. S3 of SM [58], feature **B** appears at almost the same energy in XPS and HAXPES. This indicates that the recoil effect [61] - a phenomenon observed in HAXPES of light materials [62] as a shift of the photoemission peaks to higher binding energy - is not significant. In addition, as is the case for Ni_2MnGa , the recoil effect has been reported to be insignificant for heavier 3*d* transition metal systems [49–51, 55].

It is noteworthy that according to a recent QSGW calculation [30], the austenite phase exhibits a peak right at E_F in the minority spin DOS. This is in disagreement with our present [feature a_1 in Fig. S2(a) of SM [58]] as well as previous DFT results [19, 44, 45, 63]. These DFT studies using the GGA exchange-correlation functional (XC) observed that this peak appears between -0.19 to -0.22 eV which agrees nicely with feature **A** of the HAXPES VB. In light of the good agreement between results of DFT calculation performed with GGA XC and the HAXPES data [Fig. 1], it can be argued that the GGA XC quite accurately describes the electronic structure of Ni_2MnGa . This justifies its use for our in depth investigation of the martensite phase that has complicated modulated structure with a large unit cell [14–16].

VB spectra in the Martensite phase: In the literature, the first structural refinement of Ni_2MnGa was carried out by Brown *et al.* [14] who reported $q_{\text{CDW}} = \frac{3}{7}c^*$ with sinusoidal modulations for both Ni and Mn atoms, while Ga shows a non-sinusoidal modulation [see Table S2 of SM [58] and Fig. 8b of Ref. 14]. The structure is shown in Fig. S1(b) and henceforth referred to as modulated-Brown (in short MDL-B). Righi *et al.* reported an incommensurate $q = 0.4248(2)c^*$ [see Table 1 of Ref. 15] that can be approximated to a 7-fold supercell structure [see Fig. S1(c) and Table S3 of SM [58] for structural parameters]. However, the authors estimated that their q_{CDW} is closer to $0.4c^*$ [$= \frac{2}{5}c^*$] and called it a 5M structure. In this paper, the name MDL-R has been attributed to this (modulated-Righi) structure. In contrast to MDL-B, in the MDL-R structure the amplitude and phase of modu-

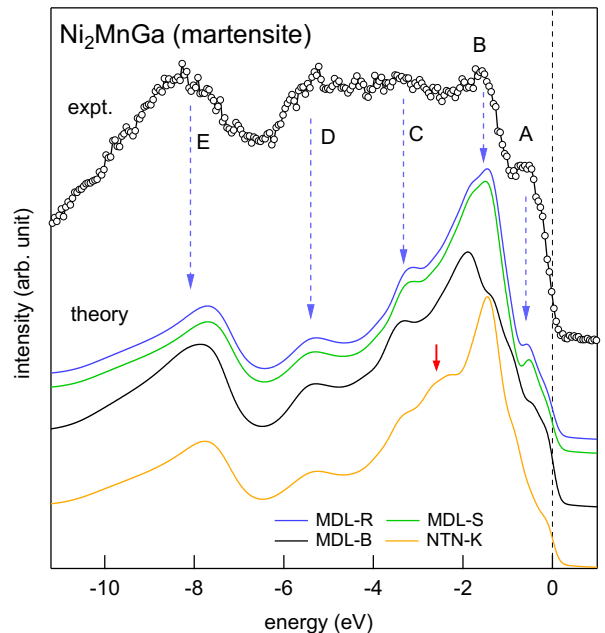


Figure 2. Theoretical VB spectra of Ni_2MnGa calculated for the different 7-fold modulated structures (MDL-R, MDL-S, and MDL-B) and the nanotwin $(5\bar{2})_2$ structure (NTN-K). These are staggered along the vertical axis and compared with the experimental VB spectrum (black open circles) in the martensite phase.

lation of all the atoms were similar [Fig. S4 of SM [58]]. Moreover, it was pointed out that the MDL-B structure contains some Ni-Mn and Ni-Ga distances – 2.09 and 2.06 Å, respectively – that are unexpectedly short [15]. In their study, Singh *et al.* found higher-order satellite reflections up to the third order and phason broadening of the satellite peaks in their XRD pattern and their refinement with the same super-space group as Righi *et al.* gave $q_{\text{CDW}} = 0.4316(3)c^*$. This was approximated to a 7-fold supercell structure with similar atomic modulations like the MDL-R structure and with a q_{CDW} value of $\frac{3}{7}c^*$ [see Table IV of Ref. 16]. This structure was referred to as 7M and is referred henceforth to as modulated-Singh (MDL-S) structure [see Fig. S1(d) and Table S4 of SM [58]]. Here, we have performed DFT calculation for all the three above discussed structures (MDL-B, MDL-R and MDL-S). We have also considered the nanotwin structure which comprises a periodic twinning, i.e. $(5\bar{2})_2$, of the tetragonal non-modulated building blocks. Since this is a model structure, we have performed a full relaxation in our DFT calculation and this is referred to as nanotwin-Kaufmann (NTN-K) structure as shown in Fig. S1(e) and the structural parameters are given in Table S5 [58].

Table 1 shows that for all the structures although both the total energy and magnetic moment are rather close to each other, the MDL-S structure has the lowest energy. The spin integrated total DOS (TDOS) and the PDOS

Table I. Formation energy (in eV/atom) and magnetic moment values (in μ_B per f.u.) obtained from DFT for different structures of Ni_2MnGa in the martensite phase.

Structure	Formation energy	Magnetic moment
MDL-B	-4.0325	3.94
MDL-R	-4.1783	4.21
MDL-S	-4.1927	4.20
NTN-K	-4.1837	4.20

for all the above mentioned structures – as well as the calculated VB along with some partial components – are shown in Figs. S5-S8 and discussed in Note B of SM [58]. In Fig. 2, we compare the calculated VB spectra for the above structures with the experiment. The suppression and shift of feature **A** to -0.55 eV in the martensite phase compared to -0.25 eV in the austenite phase [Fig. 1] in the HAXPES VB is nicely reproduced by the MDL-R and MDL-S structures [Fig. 2]. While the feature **A** is over suppressed in MDL-B, it is nearly absent in NTN-K. Further, we observe that the features close to E_F are dominated by the down spin states in case of the MDL-R and MDL-S structures, but for MDL-B and NTN-K cases, we find that these have significant contributions from both the spin channels [Fig. S2[58]]. Feature **B** is observed at the same energy position [~ -1.5 eV as shown by the blue dashed arrow] in all the structures except for MDL-B, where it is shifted considerably to about -2 eV. Thus the MDL-B structure does not show good agreement with experiment, and this could be related to the unphysically short Ni-Mn and Ni-Ga distances [15]. While features **C-E** are well reproduced in all the modulated structures, NTN-K shows an extra feature at -2.6 eV [red arrow], related to Ni 3d minority spin states, that is absent in the experiment. Thus, overall the NTN-K structure does not show good agreement indicating that the adaptive martensite model is not valid for bulk Ni_2MnGa .

From the above discussions, it is evident that the theoretical VB spectra based on the MDL-R and -S structures are in excellent agreement with the experimental results, and hence only these will be considered moving forward. In fact, the VB spectra and the DOS of these two structures are quite similar [compare Figs. S6 and S7 [58]], which is related to the closeness of their crystal structure [compare Tables S3 and S4 of SM [58]].

CDW state in the martensite phase: The top panel of Fig. 3(a) compares the experimental VB spectrum of the martensite and austenite phases. An interesting difference is observed between E_F and -1 eV: in the martensite phase, feature **A** [Fig. 1] is clearly suppressed, while an increased intensity around ~ -0.55 eV is observed in comparison to the austenite phase. However, feature **B**, as well as features **C-E** from Figs. 1,2 do not exhibit any noticeable difference. This indicates that the states close to E_F are influenced by the phase transition.

Because the thermal broadening of the Fermi func-

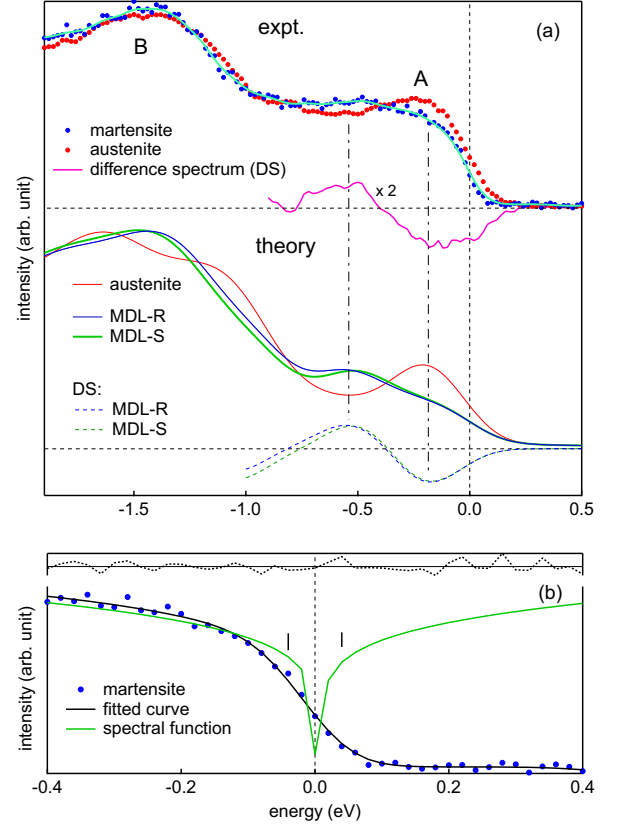


Figure 3. (a) HAXPES VB of the martensite (50 K) and austenite (300 K) phases of Ni_2MnGa in the near E_F region (top panel) taken with small data steps. The cyan curve represents the martensite spectrum thermally broadened to 300 K for comparison with the austenite phase. The bottom panel shows the theoretical VB spectra of the austenite, MDL-R and MDL-S martensite structures. Comparison of the dip and peak positions of the difference spectra (DS) between experiment (pink curve) and theory (dashed curves) shown by the dot-dashed vertical lines. (b) The martensite VB spectrum around E_F (blue filled circles) fitted (black curve) with a power law spectral function [70] (green). The residual is shown in the top panel.

tion increases with temperature, we convoluted the low temperature (50 K) martensite spectrum with a Gaussian function of full width at half maximum of $4k_B\Delta T$ [64] to obtain the difference spectra [DS = (martensite - austenite), top panel in Fig. 3(a)]. Here $\Delta T = \sqrt{T_1^2 - T_2^2}$, $T_1 = 300$ K, $T_2 = 50$ K, and k_B is the Boltzmann constant. The DS spectrum exhibits a dip centered around -0.1 eV and a peak at about -0.55 eV. This characteristic dip-peak shape points to a transfer of spectral weight from -0.1 eV to -0.55 eV, which is known to be a manifestation of the CDW state that has been observed in other systems [65–68]. In addition, the suppression of states at E_F supports the emergence of a pseudogap, as would be anticipated for a CDW state [6, 8]. In order to confirm this, the shape of the spectrum near

E_F needs to be determined because, according to the theoretical formulation of CDW [6, 69], it should follow a power law function [70] where α is the exponent. This function was used to fit the near E_F spectrum of the martensite phase using a least-square error minimization approach, where multiple starting values were applied and all parameters were adjusted, with the exception of the instrumental resolution. A random variation of the residual in the top panel of Fig. 3(b) shows that the fitting is satisfactory.

Interestingly, the power law function portrays the pseudogap at E_F , and its width is estimated to be 80 meV from the separation between the inflection points shown by the black ticks. α determines the shape of the spectral function, its value turns out to be 0.18 ± 0.02 , which is close to that reported (0.16) for the surface CDW of Ni_2MnGa in the martensite phase probed using surface-sensitive ($<5\text{\AA}$) UPS [13]. This shows that the CDW has similar nature in the bulk and the surface. This is also supported by the similarity of q_{CDW} value obtained from the surface sensitive low energy electron diffraction study [25] and the bulk value from XRD.

Having shown in Fig. 2 that the MDL-R and -S structures best describe the position of all the features **A-E** of the experimental VB spectrum in the martensite phase, we address the question whether the transfer of spectral weight is observed from theory. Indeed, an excellent agreement of the dip and peak positions of the DS between experiment and theory has been observed, which is revealed by the dot-dashed vertical lines in Fig. 3(a).

Conclusion: We have investigated the bulk electronic structure of stoichiometric Ni_2MnGa employing DFT and HAXPES to show the existence of CDW in the martensite phase. To this end, at the onset, the VB calculated by DFT for the austenite phase with a simple cubic L2_1 structure is compared with the HAXPES VB. The energy positions of all the features in the experimental spectrum are in excellent agreement with the calculated VB spectrum validating the efficacy of the GGA exchange-correlation functional for describing the electronic structure of Ni_2MnGa . For the martensite phase, to the best of our knowledge, no electronic structure calculation exists for the modulated structures reported by structural refinement of neutron or x-ray diffraction data. We have calculated the spin-polarized DOS and PDOS for three such structures: MDL-B [14], MDL-R [15] and

MDL-S [16]. Furthermore, the nanotwin model structure (NTN-K) [28] with a $(52)_2$ stacking that was suggested by the adaptive model was considered. Comparison of the theoretical VB spectra obtained for the above mentioned MDL-R [15] and MDL-S [16] structures, with the HAXPES data, showed a very good feature to feature agreement in peak intensity and positions, indicating existence of modulation and CDW in the martensite phase. On the other hand, the NTN-K structure did not show good agreement indicating that the adaptive martensite model is not valid for bulk Ni_2MnGa .

The VB DOS in the martensite phase is suppressed at E_F compared to the austenite phase. By fitting the near E_F region with a power law function, we identify a pseudogap of about 80 meV width. Concomitantly, a spectral weight transfer occurs from the near E_F region to the higher binding energy side, resulting in a dip-peak structure in the difference spectrum [between austenite and martensite phases]. These two observations establish the existence of CDW in Ni_2MnGa . The excellent agreement in the difference spectra between experiment and the theory for the 7-fold modulated MDL-R and -S structures show the role of the periodic atomic modulation in achieving the CDW state. Our combined DFT and HAXPES study establishes for the first time a CDW driven electronic origin of the martensite phase transition in bulk Ni_2MnGa .

Acknowledgments: JB and AC thank the director, RRCAT for facilities and encouragement, and A. Banerjee and T. Ganguli for discussion. RRCAT computer division is thanked for the installation of the softwares and support. JB thanks RRCAT and HBNI for financial support. The HAXPES experiments were carried out at PETRA III of Deutsches Elektronen-Synchrotron, a member of Helmholtz-Gemeinschaft Deutscher Forschungszentren. Financial support by the Department of Science and Technology, Government of India within the framework of India@DESY collaboration is gratefully acknowledged. T. A. Lograsso and D. L. Schlagel are thanked for providing us with the single crystal specimen. We are thankful to C. Schlueter and K. Biswas for support and encouragement. We would like to acknowledge the skillful technical support from K. Ederer.

-
- [1] Y. Wang *et al.*, Nature **606**, 896 (2022).
 - [2] H. Pan, M. Xie, F. Wu, and S. Das Sarma, Phys. Rev. Lett. **129**, 056804 (2022).
 - [3] Y.-X. Jiang *et al.*, Nature Materials **20**, 1353 (2021).
 - [4] W. Shi *et al.*, Nature Physics **17**, 381 (2021).
 - [5] A. Zong *et al.*, Nature Physics **15**, 27 (2018).
 - [6] R. H. McKenzie, Phys. Rev. B **52**, 16428 (1995).
 - [7] G. Grüner, Rev. Mod. Phys. **60**, 1129 (1988).
 - [8] P. A. Lee, T. M. Rice, and P. W. Anderson, Phys. Rev. Lett. **31**, 462 (1973).
 - [9] P. Walmsley, S. Aeschlimann, J. A. W. Straquadine, P. Giraldo-Gallo, S. C. Riggs, M. K. Chan, R. D. McDonald, and I. R. Fisher, Phys. Rev. B **102**, 045150 (2020).
 - [10] J. Dai, E. Calleja, J. Alldredge, X. Zhu, L. Li, W. Lu, Y. Sun, T. Wolf, H. Berger, and K. McElroy, Phys. Rev. B **89**, 165140 (2014).
 - [11] H. J. Kim, C. D. Malliakas, A. T. Tomić, S. H. Tessmer, M. G. Kanatzidis, and S. J. L. Billinge, Phys. Rev. Lett.

- 96**, 226401 (2006).
- [12] C. Phatak, O. Heinonen, M. D. Graef, and A. P.-Long, *Nano Lett.* **16**, 4141 (2016).
 - [13] S.W. D'Souza, A. Rai, J. Nayak, M. Maniraj, R. S. Dhaka, S. R. Barman, D. L. Schlagel, T. A. Lograsso, and A. Chakrabarti, *Phys. Rev. B* **85**, 085123 (2012).
 - [14] P. J. Brown, J. Crangle, T. Kanomata, M. Matsumoto, K. -U. Neumann, B. Ouladdiaf, and K. R. A. Ziebeck, *J. Phys.: Cond. Mat.* **14**, 10159 (2002).
 - [15] L. Righi, F. Albertini, G. Calestani, L. Pareti, A. Paoluzi, C. Ritter, P. A. Algarabel, L. Morellon, and M. R. Ibarra, *J. Solid State Chem.* **179**, 3525 (2006).
 - [16] S. Singh, V. Petricek, P. Rajput, A. H. Hill, E. Suard, S. R. Barman, and D. Pandey, *Phys. Rev. B* **90**, 014109 (2014).
 - [17] V. V. Martynov and V. V. Kokorin, *J. Phys. III France* **2**, 739 (1992).
 - [18] C. Bungaro, K. M. Rabe, and A. Dal Corso, *Phys. Rev. B* **68**, 134104 (2003).
 - [19] A. T. Zayak, P. Entel, J. Enkovaara, A. Ayuela, and R. M. Nieminen, *J. Phys.: Cond. Mat.* **15**, 159 (2003).
 - [20] S. M. Shapiro, P. Vorderwisch, K. Habicht, K. Hradil, and H. Schneider, *Europhys. Lett.* **77**, 56004 (2007).
 - [21] A. Zheludev, S. M. Shapiro, P. Wochner, and L. E. Tanner, *Phys. Rev. B* **54**, 15045 (1996).
 - [22] R. Chulist, C. -G. Oertel, W. Skrotzka, and T. Lippmann, *Scripta Materialia* **62** 235 (2010).
 - [23] S. O. Mariager, C. Dornes, J. A. Johnson, A. Ferrer, S. Greubel, T. Huber, A. Caviezel, S. L. Johnson, T. Eichhorn, G. Jakob, H. J. Elmers, P. Beaud, C. Quitmann, and G. Ingold, *Phys. Rev. B* **90**, 161103(R) (2014).
 - [24] S. Singh, J. Bednarcik, S. R. Barman, C. Felser, and D. Pandey, *Phys. Rev. B* **92**, 054112 (2015).
 - [25] S. W. D'Souza, J. Nayak, M. Maniraj, A. Rai, R. S. Dhaka, S. R. Barman, D. L. Schlagel, T. A. Lograsso, and A. Chakrabarti, *Surf. Sci.* **606**, 130 (2012).
 - [26] T. Fukuda, H. Kishida, M. Todai, T. Kakeshita, and H. Mori, *Scr. Mater.* **61**, 473 (2009).
 - [27] J. Pons, R. Santamarta, V. A. Chernenko, and E. Cesari, *J. Appl. Phys.* **97**, 083516 (2005).
 - [28] S. Kaufmann, U. K. Röbler, O. Heczko, M. Wuttig, J. Buschbeck, L. Schultz, and S. Fähler, *Phys. Rev. Lett.* **104**, 145702 (2010).
 - [29] M. E. Gruner, R. Niemann, P. Entel, R. Pentcheva, U. K. Rössler, K. Nielsch, and S. Fähler, *Sci. Rep.* **8**, 8489 (2018).
 - [30] M. Obata, T. Kotani, and T. Oda, *Phys. Rev. Mater.* **7**, 024413 (2023).
 - [31] X. Zhou, W. Li, H. P. Kunkel, and G. Williams, *J. Phys.: Cond. Mat.* **16**, L39 (2004).
 - [32] J. Marcos, L. Mañosa, A. Planes, F. Casanova, X. Batlle, and A. Labarta, *Phys. Rev. B* **68**, 094401 (2003).
 - [33] A. Sozinov, A. A. Likhachev, N. Lanska, and K. Ullakko, *Appl. Phys. Lett.* **80**, 1746 (2002).
 - [34] S. J. Murray, M. Marioni, S. M. Allen, R. C. O'Handley, and T. A. Lograsso, *Appl. Phys. Lett.* **77**, 886 (2000).
 - [35] F. Casoli, G. Varvaro, M. T. Ghahfarokhi, S. Fabbri and F. Albertini, *J. Phys.: Materials* **3**, 045003 (2020).
 - [36] E. DiMasi, M. C. Aronson, J. F. Mansfield, B. Foran, and S. Lee, *Phys. Rev. B* **52**, 14516 (1995).
 - [37] S. Sarkar *et al.* arXiv:2212.01181
 - [38] S. Singh, J. Nayak, A. Rai, P. Rajput, A. H. Hill, S. R. Barman, and D. Pandey, *J. Phys.: Cond. Mat.* **25**, 212203 (2013).
 - [39] Y. Sokolovskaya, O. Miroshkina, D. Baigutlin, V. Sokolovskiy, M. Zagrebin, V. Buchelnikov, and A. T. Zayak, *Metals* **11**, 973 (2021).
 - [40] A. N. Vasilev, A. D. Bozhko, V. V. Khovailo, I. E. Dikshtein, V. G. Shavrov, V. D. Buchelnikov, M. Matsumoto, S. Suzuki, T. Takagi and J. Tani, *Phys. Rev. B* **59**, 1113 (1999).
 - [41] S. Banik, R. Ranjan, A. Chakrabarti, S. Bhardwaj, N. P. Lalla, A. M. Awasthi, V. Sathe, D. M. Phase, P. K. Mukhopadhyay, D. Pandey, and S. R. Barman, *Phys. Rev. B* **75**, 104107 (2007).
 - [42] S. Banik, S. Singh, R. Rawat, P. K. Mukhopadhyay, B. L. Ahuja, A. M. Awasthi, S. R. Barman, and E. V. Sampathkumaran, *J. Appl. Phys.* **106**, 103919 (2009).
 - [43] S. W. D'Souza, R. S. Dhaka, A. Rai, M. Maniraj, J. Nayak, S. Singh, D. L. Schlagel, T. A. Lograsso, A. Chakrabarti, and S. R. Barman, *Mater. Sci. Forum* **684**, 215 (2011).
 - [44] S. Fujii, S. Ishida, and S. Asano, *J. Phy. Soc. Japan* **58**, 3657 (1989).
 - [45] S. R. Barman, S. Banik, and A. Chakrabarti, *Phys. Rev. B* **72**, 184410 (2005).
 - [46] S. Shin, *AAPPS Bull.* **31**, 21 (2021).
 - [47] *Hard X-ray Photoelectron Spectroscopy*, ed. J. C. Woicik, Springer Series in Surface Sciences vol. **59** (Springer International Publishing, Switzerland, 2016).
 - [48] A. X. Gray *et al.*, *Nat. Mater.* **10**, 759 (2011); *Nat. Mater.* **11**, 958 (2012); *Phys. Rev. Lett.* **108**, 257208 (2012); T. Ohtsuki *et al.*, *Phys. Rev. Lett.* **106**, 047602 (2011); M. Sing *et al.*, *Phys. Rev. Lett.* **102**, 176805 (2009).
 - [49] J. Nayak, M. Maniraj, A. Rai, S. Singh, P. Rajput, A. Gloskovskii, J. Zegenhagen, D. L. Schlagel, T. A. Lograsso, K. Horn, and S. R. Barman, *Phys. Rev. Lett.* **109**, 216403 (2012).
 - [50] V. K. Singh, M. Krajčí, S. Sarkar, M. Balal, S. Barman, P. Sadhukhan, A. Gloskovskii, M. Feuerbacher, C. Thomas, P. Ebert, E. Rotenberg, K. Horn, and S. R. Barman, *Phys. Rev. B* **105**, 205107 (2022).
 - [51] S. Sarkar, P. Sadhukhan, V. K. Singh, A. Gloskovskii, K. Deguchi, N. Fujita, and S. R. Barman, *Phys. Rev. Res.* **3**, 013151 (2021).
 - [52] P. Sadhukhan, S. W. D'Souza, V. K. Singh, R. S. Dhaka, A. Gloskovskii, S. K. Dhar, P. Raychaudhuri, A. Chainani, A. Chakrabarti, and S. R. Barman, *Phys. Rev. B* **99**, 035102 (2019).
 - [53] M. Ye, A. Kimura, Y. Miura, M. Shirai, Y. T. Cui, K. Shimada, H. Namatame, M. Taniguchi, S. Ueda, K. Kobayashi, R. Kainuma, T. Shishido, K. Fukushima, and T. Kanomata, *Phys. Rev. Lett.* **104**, 176401 (2010).
 - [54] S. Ueda, Y. Miura, Y. Fujita, and Y. Sakuraba, *Phys. Rev. B* **106**, 075101 (2022).
 - [55] P. Sadhukhan, S. Sarkar, S. W. D'Souza, A. Gloskovskii, and S. R. Barman, *Physica Scripta* (accepted).
 - [56] A. Kimura, M. Ye, M. Taniguchi, E. Ikenaga, J. M. Barandiarán, and V. A. Chernenko, *Appl. Phys. Lett.* **103**, 072403 (2013).
 - [57] P. J. Webster, K. R. A. Ziebeck, S. L. Town, and M. S. Peak, *Philos. Mag. B* **49**, 295 (1984).
 - [58] See Supplemental Material at xx.xx
 - [59] S. Tanuma, C. J. Powell, and D. R. Penn, *Surf. Intf. Anal.* **43**, 689 (2011). C. J. Powell, A. Jablonski, I. S. Tilinin, S. Tanuma, and D. R. Penn, *J. Electron Spectros. Relat. Phenom.* **98-99**, 1 (1999).
 - [60] M.B. Trzhaskovskaya, and V.G. Yarzhevsky, *Atomic*

- Data Nucl. Data Tables **119**, 99 (2018).
- [61] C. Fadley, J. Electron Spectrosc. Relat. Phenom. **178-179**, 2 (2010).
- [62] Y. Takata, *et al.*, Phys. Rev. B **75**, 233404 (2007); Phys. Rev. Lett. **101** 137601 (2008).
- [63] A. Ayuela, J. Enkovaara, K. Ullakko, and R. M. Nieminen, J. Phys.: Cond. Matt. **11**, 2017 (1999).
- [64] A. Singh, H. Y. Huang, Y. Y. Chin, Y. F. Liao, T. C. Huang, J. Okamoto, W. B. Wu, H. J. Lin, K. D. Tsuei, R. P. Wang, F. M. F. de Groot, C. N. Kuo, H. F. Liu, C. S. Lue, C. T. Chen, D. J. Huang, and A. Chainani, Phys. Rev. B **98**, 235136 (2018).
- [65] B. Dardel, D. Malterre, M. Grioni, P. Weibel, Y. Baer, and F. Levy, Phys. Rev. Lett. **67**, 3144 (1991).
- [66] B. Dardel, M. Grioni, D. Malterre, P. Weibel, Y. Baer, and F. Levy, Phys. Rev. B **46**, 7407 (1992).
- [67] J. Matsuno, A. Fujimori, L. F. Mattheiss, R. Endoh, and S. Nagata, Phys. Rev. B **64**, 115116 (2001).
- [68] T. Yokoya, T. Kiss, A. Chainani, S. Shin, and K. Yamaya, Phys. Rev. B **71**, 140504(R) (2005).
- [69] C. A. Balseiro, P. Schlottmann, and F. Yndurain, Phys. Rev. B **21**, 5267 (1980).
- [70] unit step function, α is the exponent of the power law function, and w is a multiplicative factor. $f(E, T)$ represents the Fermi function at temperature T .
- [71] G. Kresse and J. Furthmüller, Phys. Rev. B **54**, 11169 (1996); G. Kresse and D. Joubert, Phys. Rev. B **59**, 1758 (1999).
- [72] J. P. Perdew, K. Burke, and M. Ernzerhof, Phys. Rev. Lett. **77**, 3865 (1996).
- [73] H. J. Monkhorst and J. D. Pack, Phys. Rev. B **13**, 5188 (1976).
- [74] A. Gloskovskii, G. Stryganyuk, G. H. Fecher, C. Felser, S. Thiess, H. Schulz-Ritter, W. Drube, G. Berner, M. Sing, R. Claessen, and M. Yamamoto, J. Electron Spectrosc. Relat. Phenom. **185**, 47 (2012).
- [75] D. L. Schlagel, Y. L. Wu, W. Zhang, and T. A. Lograsso, J. Alloys Compd. **312**, 77 (2000).
- [76] R. S. Dhaka, S. W. D'Souza, M. Maniraj, A. Chakrabarti, D. L. Schlagel, T. A. Lograsso, and S. R. Barman, Surf. Sci. **603** 1999 (2009).
- [77] D. A. Shirley, Phys. Rev. B **5**, 4709 (1972).
- [78] A. Chakrabarti, M. Siewert, T. Roy, K. Mondal, A. Banerjee, M. E. Gruner, and P. Entel, Phys. Rev. B **88**, 174116 (2013); A. T. Zayak, P. Entel, K. M. Rabe, W. A. Adeagbo, and M. Acet, Phys. Rev. B **72**, 054113 (2005).
- [79] A. Chakrabarti, C. Biswas, S. Banik, R. S. Dhaka, A. K. Shukla, and S. R. Barman, Phys. Rev. B **72**, 073103 (2005).
- [80] K. Momma and F. Izumi, J. Appl. Crystallogr. **44**, 1272 (2011).

$$[w \times f(E, T) \times [|E - E_0|^\alpha] h(E - E_0) + |E'_0 - E|^\alpha h(E'_0 - E)] \otimes (E, \sigma) \quad (1)$$

where E_0 (E'_0) is the threshold energy of the left (right) branch of the power law spectral function, h denotes a